Biol. Cybern. 80, 117–129 (1999)

Biological Cybernetics

Cortical hypercolumn size determines stereo fusion limits

Yehezkel Yeshurun[1], Eric L. Schwartz[2]

[1]Department of Computer Science, School of Mathematics, Tel Aviv University, Ramat Aviv, Israel 69978
[2]Department of Cognitive and Neural Systems, Boston University, Boston, Mass., 02146, USA

Received: 2 December 1991 / Accepted in revised form: 18 September 1998

Abstract. The size of a pair of cortical ocular dominance columns determines a basic anatomical module of V-1 which Hubel and Wiesel have termed the hypercolumn. *Does this correspond to a basic functional, or psychophysically measurable, module as well?* This is the basic question addressed in the present paper. Since the ocular dominance column architecture is presumed to be related to stereo vision, it is natural to assume that hypercolumn size should provide a modular basis for basic phenomena of stereopsis. In previous work, we have suggested that local nonlinear filtering via the cepstral transform, operating on a local window of cortical tissue scaled by hypercolumn size, provides such a modular model of stereopsis. In the present paper, we review this model and then discuss a number of issues related to the biological plausibility and implementation of this algorithm. Then, we present the main result of this paper: we have analyzed a number of experiments related to stereo fusion limits (Panum's area) and to disparity gradient and disparity scaling, and demonstrate that there is a simple unifying explanation for these phenomena in terms of a constant cortical module whose size is determined by a pair of ocular dominance columns. As a corollary, Panum's area must increase according to (inverse) cortical magnification factor. We show that this is supported by all existing experimental data.

1 Introduction

In his classical study of stereopsis, K. Ogle (1952) commented: "The fact that a defined range of disparities exists within which the perception of stereoscopic depth occurs is evidence of neuroanatomic limitations ... These [limitations] could be accounted for by the extent to which the neural paths that arise at the retinas of the two eyes ... overlap at the occipital cortex ..."

Correspondence to: E.L. Schwartz

In modern terms, the question raised by Ogle's remarks may be addressed in terms of the functional architecture of the primary visual cortex. What are the joint effects of cortical topography and columnar architecture on the psychophysical phenomena of stereopsis? If, following the original suggestion of Hubel and Wiesel (1974), we take the basic module of the striate cortical architecture to be a "hypercolumn", which was defined to be equal to the size of a left-right pair of ocular dominance columns, then we seek to investigate the role of this basic constant, together with the effects of cortical topography, on stereo vision.

Schwartz (1977a) suggested that Panum's area is determined by the size of cortical hypercolumns, and that it should then scale with the cortical magnification factor. This hypothesis provides a tentative answer to Ogle's original suggestion, quoted at the beginning of this paper.

Many psychophysical phenomena have been observed to scale, at least approximately, as a linear function of visual field eccentricity (Virsu and Rovamo 1979). The slope and intercept of such a linear function might be related to the parameters of other scaling laws, such as retinal cell density, or cortical magnification. If so, this type of observation provides a possible insight into the anatomical correlates of the given psychophysical phenomena.

In the present paper, we examine the relationship of cortical scaling, and more specifically, the role of hypercolumn size, to stereo fusion and disparity representation. A major problem in this area is related to the range of estimated magnification functions in monkey and human. At least two major issues cloud this area. The first is that aside from some recent coarse estimates based on positron emission tomography (PET) and functional magnetic resonance imaging (fMRI), there is no reliable direct measurement of human magnification factor available. Rather, monkey data, based on microelectrode recording and 2DG imaging studies, provides a data source, but one which is still clouded by measurement uncertainties. The difficulty in this area is underlined by the lack of "error bars" or error analysis in the primate topography literature, making it difficult

to provide a confidence limit on any statements in this area. This situation is now improving, and recently it has been possible to obtain an estimate of the two-dimensional (2D) conformal map structure of macaque visual topography, using 2DG imaging and computer brain flattening methods. This fit appears to be accurate to within roughly 20% (Schwartz 1994). We will return to the discussion of the current level of understanding of monkey and human visual topography later in this paper.

There are at least two basic spatial scales associated with early vision, which we call λ_H (about 5 arc-s, hyperacuity) and λ_R (.5–1 arc-min, maximal visual acuity). To these, we suggest adding a third basic scale, which we call λ_C, determined by the size of hypercolumns in V-1 and cortical magnification factor. We show in this paper that λ_C is associated with the scaling of Panum's area for stereo fusion and several recent results in motion perception. We estimate it to be roughly 8–16 arc-min in the central fovea, scaling linearly with inverse cortical magnification factor.

We present the motivation for the current paper by briefly discussing the biological plausibility of a computational model of stereopsis (Yeshurun and Schwartz 1989). This model is based on the idea of using a local, nonlinear correlational operator (cepstrum), on fixed "windows" whose size is determined by the ocular dominance column scale. We then discuss various psychophysical findings pertaining to stereopsis, including the scaling of Panum's area (Schor et al. 1989) and the disparity gradient experiment of (Burt and Julesz 1980). We show that these experiments are consistent with the notion of a fixed size cortical processing module. One side effect of this analysis is to re-instate the concept of Panum's area as a valid one, despite these latter two experiments, which have been interpreted as contradicting the significance, or even the existence, of a specific Panum's area.

2 Computational and biological background of cepstral correlation

In this section, we

- Review the basic statement of the cepstral stereo algorithm.
- State the features of cepstral stereo in the context of biological stereo vision.
- Provide a brief intuitive explanation of both the cepstral operator and the related phase-only filter algorithm.
- Briefly discuss the neural plausibility of algorithms based on power spectral estimation.
- Indicate a generic problem, and solution, to the biological plausibility of any algorithm which is based on "square-law" or correlation "energy".

Following this section, we then present the main point of this paper, which is that local correlation on a fixed window size, which is determined by the ocular dominance column size in V-1 and the magnitude of cortical magnification factor, is consistent with known psychophysical, physiological, and anatomical estimates. This observation is supported with a clarification and resolution of some conflicting experimental work on Panum's fusional area and recent experimental work on motion perception.

2.1 The cepstral operator

Consider the following statement of the stereo problem: two slightly different images are spatially organized side by side, in the form of small "patches" of left eye and right eye input. This pattern of interlacing of stereo images is similar to that which is found in layer IV of primate visual cortex. We would like to apply a spatial filter to the "combined" left-right image, such that its output is the relative shift, or disparity, between the projection of an object in the two half-images.

To illustrate this idea, consider an interlaced image $f(x,y)$ that is composed of a single columnar (left-right) pair. Also, assume that the data consist of an image patch $s(x,y)$ (the "right image") and a shifted patch "butted" against it (the left image) as shown in Fig. 1. The interlaced image can be represented as follows. (The $\otimes$ operator represents 2D convolution.)

$$f(x,y) = s(x,y) \otimes (\delta(x,y) + \delta(x-D,y)) \tag{1}$$

The Fourier transform of such an image pair is

$$F(u,v) = S(u,v) \cdot (1 + e^{-i\pi(D \cdot u)}) \tag{2}$$

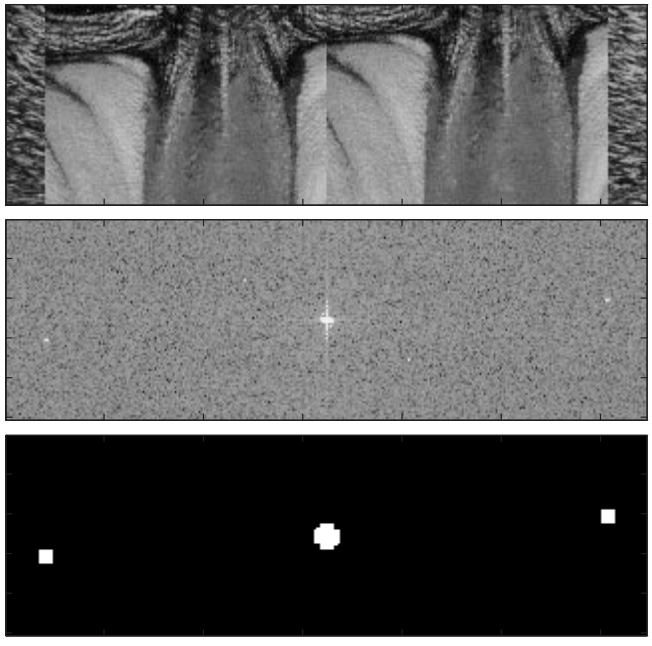

Fig. 1. *Top* A pair of image patches. There is both horizontal and vertical disparity. *Middle* The cepstrum of the image. *Bottom* The cepstrum image intensities are thresholded for demonstration purposes. The origin of the frequency plane has been shifted to the center of the frame. The disparity terms occur as bright spots in the cepstrum

By forming the logarithm of $F(u,v)$, the product structure becomes a sum:

$$\log F(u,v) = \log S(u,v) + \log(1 + e^{-i\pi D \cdot u}) \quad (3)$$

The power spectrum of (3) (see Figure 1) will have a prominent term located at the magnitude of the shift $(D,0)$. The operator derived from this description, namely, the power spectrum of the log of the power spectrum (denoted "cepstrum"), was originally analyzed by Bogert et al. (1963) and has since been widely used in 1D signal processing. Recently, interest has been growing in the application of the 2D generalization of the cepstrum to both stereo and motion correlation applications (Lee et al. 1989; Ludwig et al. 1994; Yeshurun and Schwartz 1989). One common application of cepstral filtering is for echo detection. An echo is a shifted version of a signal, and since the cepstrum provides the echo's delay, it is possible to remove the echo by means of the inverse transform. With reference to Fig. 1, the quantity of interest is the delay (i.e., the disparity) and not the signal per se. Note that the cepstral transform of (3), which is the result of two successive power spectral transforms, is expressed in spatial units. Thus, the shift (D,0), which shows up as a bright peak in the cepstral domain (actually two peaks, due to symmetry), has units of angular (i.e., spatial) disparity. A simple peak detection algorithm can measure the binocular disparity directly from the cepstrum of the columnar image pair, in the same spatial (i.e. angular) units as the underlying visual map. In other words, the cepstrum provides a spatial map of disparity.

2.2 Computational properties of the cepstrum and the phase-only filter

The phase-only filter (POF) has been suggested as a computational basis for stereo (Jenkin and Jepson 1989), and the POF has also been considered by Olson and Potter (1988) in the context of computer vision applications and directly compared by them to cepstral stereo. In the context of computer vision, Olson and Potter found the cepstral approach to be more efficient.

To clarify this issue and its relation to possible biological implementation, we feel that it is useful to present here some intuitive insights into the nature of both cepstral and POF stereo algorithms which may be useful in understanding how these two approaches related, and why they work well in the first place.

The POF is a correlational or template matching algorithm which performs frequency domain matching by the multiplication of the modified Fourier transform of two images. As is well known, the Fourier transform of the correlation of two images is given by the product of the Fourier transforms of each image (Bracewell 1978). The POF method sets all amplitudes in both Fourier transforms to unity, prior to multiplying the transforms. The empirical justification for this is the observation that the POF provides very good localization of stereo peaks. The POF has seen a wide area of application in optical computing in general and following Jenkin and Jepson (1989), has been suggested for stereo matching.

We address three issues in regard to the POF and the cepstrum:

1. What is the intuitive basis of the POF?

   By setting the amplitude of all frequency components to unity, the POF effectively performs a high-pass filter. This is because the natural spectrum of images usually follows a $1/f$ amplitude structure: high frequencies tend to have small amplitudes. By equating all amplitudes, the POF tends to boost the amplitude of the high frequency part of the spectrum. This yields good positional estimates since the low frequency components are de-emphasized.
2. What is the relationship of the POF to the cepstrum?

   The cepstrum differs from conventional cross-correlation by the use of a logarithmic transformation of the image power spectrum. The logarithmic transformation is "compressive": the large amplitude components of the spectrum, which tend to be in the low-frequency component of the spectrum, are de-emphasized. In a sense, the cepstrum, like the POF, can be seen as a nonlinear high-pass filter based on the compressive nature of the logarithm.

   Although by no means identical, the cepstral and POF approaches share the common property of boosting the high-frequency relative to the low-frequency components of the spectrum, under the assumption, as is often the case, that the spectrum scales like $1/f$.
3. What are the computational and biological plausibility of both approaches?

   In computational terms, Olson and Potter (1988) have provided a detailed analysis of the POF versus the cepstrum in a stereo matching application. They concluded that the cepstrum is more efficient to compute via the use of the fast Fourier transform (FFT) and claim that both give similar practical performance.

   The cepstrum requires access only to the power spectrum (of the binocular interlaced image) and not to the phase spectrum. The POF requires access only to the phase spectrum and not to the power spectrum. The question of whether cortical neurons provide a representation of the phase spectrum is, at present, unclear. However, the question of whether cortical neurons provide power-spectral estimates is certain and affirmative. Cortical neurons are widely recognized as medium band width power spectral filters. In this sense, the cepstral filtering approach is better justified than the POF, in the context of the current understanding of the central nervous system.

   Finally, the cepstral method, in addition to the requirement of power-spectral estimates, requires a logarithmic (compressive) nonlinearity. In our earlier work, we suggested that a logarithmic transfer function is a widely observed property of sensory neurons

(Yeshurun and Schwartz 1989). Recently, it has become clear that a compressive nonlinearity similar to the logarithm is provided generically by the integrate-and-fire model of neuronal transduction (Tal and Schwartz 1997). Thus, both the power spectral estimating and compressive logarithmic transfer functions required by the cepstrum are basic, firmly established properties of neurons. Phase representation and manipulation of the type required by the POF are not well established as neuronal properties at the present time.

2.3 Performance issues of cepstral filtering

In addition to a favorable signal-to-noise ratio, the cepstral operator has good "robustness" to image degradation, which is similar to psychophysical studies of human stereopsis (see (Julesz 1971) demonstrating a remarkable resistance to various image degradations, rotations, and expansions. It is possible to differentially expand (up to 15%), to rotate (up to 6 deg), to blur (with a Gaussian), to add random noise, and to change image intensity (e.g., by histogram equalization) of one half-image with respect to the other, without disrupting the cepstral disparity estimation (Yeshurun and Schwartz 1989). For these distortions, the disparity peak is no longer concentrated in a single point, but rather "smeared" over a small region. Yet its centroid is easily detected and provides an estimate of disparity which is accurate to sub-pixel precision (Yeshurun and Schwartz 1989), and hence provides a stereo-acuity threshold which can be one or two orders of magnitude smaller than the window size. These robustness properties are not shared by typical "pixel-matching" computational algorithms, which tend to fail ungracefully when the stereo-pairs depart from a simple shifted copy of one another. In fact, it is often stated that there is a fundamental difficulty with scene matching algorithms, in that false localization of targets can occur (Julesz 1971). This problem disappears when a locally windowed cepstral (or other correlational) approach is used: peak detection applied to a windowed algorithm quite naturally provides a single disparity value for the entire window. However, if multiple peaks are sought (Weinshall 1989), then it could be carried out by a variety of signal processing techniques.

2.4 Power spectral estimation by medium band width neuronal filters and the square-law detectors in biological correlation applications

Since the behavior of the windowed cepstral stereo algorithm is in good agreement, both qualitatively and quantitatively, with a wide range of properties of human stereo, we now focus our attention on the details of biological implementation of a windowed cepstral filter. The two questions that we address in this section are:

- Is it feasible for medium band-width spatial filters, of the type associated with V-1 receptive fields, to form the basis of a cepstral filter with sufficient precision to support the details of stereo-acuity?
- Correlational algorithms have identical performance if one of the stereo images is inverted in contrast. But humans cannot fuse positive-negative random dot stereograms. On the other hand, they can fuse positive-negative line drawings (Julesz 1971). Are these properties of human stereopsis consistent with a cepstral, or other, correlational operator?

2.5 Neural power spectral density estimation

The power spectral and cepstral figures in our previous work were produced using a conventional digital FFT. This is not a particularly biological computation, to say the least. It initially seemed to us and to others (e.g. Blake and Wilson 1991) that the medium band width spatial-filtering properties of cortical neurons are too coarse to support a cepstral stereo estimation. This issue is of some significance because of the important role of spatial frequency processing in psychophysics and visual physiology. However, with the exception of the work of Okajima (1986), there has been relatively little computational use made of neural spatial filters for correlation. Therefore, the first question that we address is whether the use of the medium band width spatial-filtering properties of cortical neurons, rather than a digital FFT, would be sufficient to produce a usable cepstral peak in the stereo scenes which we have analyzed.

Estimation of power spectrum by Gabor-type "receptive fields" is known to be achievable. Turner (1986) showed that it is possible to estimate power spectra with sufficient accuracy to carry out texture segmentation. We are currently investigating the plausibility of a full-scale estimation of the cepstrum by a receptive field model, and preliminary results show that it is possible to estimate it with sufficient resolution, using a set of medium bandwidth filters (simulating cortical receptive fields). Thus, at the present time, we have reason to believe that the medium band-width tuning properties of cortical neurons are consistent with useful power-spectral estimation, both for cepstral and for conventional textural applications.

3. "Square law" stereo detectors and "positive-negative" stereogram

Windowed correlational mechanisms for stereo are robust and do not suffer from the so-called correspondence problem (Julesz 1971; Marr 1982) since a windowed operator, together with "peak detection", can naturally provide only a single value per window[1].However, these methods are generally based on a "square

[1]As noted earlier, by generalizing the peak detection algorithm, a small number of peaks could be accommodated. However, the huge number of false correspondences described by Julesz (1971) and Marr (1982) is avoided by any windowed stereo algorithm.

law'', or energy-based detection. The cross-correlation, or the cepstrum, of two adjacent scene patches is computed from a ''magnitude'', or energy, and so is unchanged if one of the two scenes becomes negated in contrast. In psychophysical terms, humans can fuse positive-negative line stereograms, with a rivalrous percept (Julesz, 1971), but cannot fuse positive-negative random dot stereograms. It would seem that ''square-law'', or energy-based measures would have to be excluded for human vision, due to this basic asymmetry in the nature of the correlation between left and right scenes (for random dot stereograms), because, as depicted in Fig. 2, a random dot stereogram would be equally well solved by the cepstrum if one of the half-images was inverted in contrast. However, a symmetry-breaking mechanism exists in primate visual systems which is based on the segregation of the ON-OFF and OFF-ON mechanisms in the retina, lateral geniculate nucleus (LGN) and visual cortex (Schiller 1983).

A simple rationale for the existence of separate OFF-ON and ON-OFF channels is based on the single-ended nature of the neural response: for neurons to signify both positive and negative contrast, there would need to be a high resting spontaneous discharge rate, to allow a bipolar swing about zero contrast. The low spontaneous discharge rate typical of the visual cortex, which is obviously advantageous in metabolic terms, if not in computational terms, requires two separate systems of rectified signals to represent a bipolar contrast range (see Schiller, 1983). In order to explore the symmetry-breaking aspects of separate ON-OFF and OFF-ON systems, we simulated a cepstral-filtered stereo algorithm on such separate inputs. Instead of using the intensity image as the input, we have used directional edge information that represents the ON-OFF image and the OFF-ON image. This is simulated as follows: the (retinal) image is passed through a directional edge detector, and this filtered image is then used as the input for the cepstrum. The results indicated that the cepstrum is not sensitive to intensity reversal. As expected, the cepstrum is a ''square-law'' based detector.

However, if the image is filtered by an ON-OFF (and OFF-ON) layer then not only the intensity is changed but also the spatial location of the patterns. Suppose that the grey level image consists of a vertical light bar on a dark background: the OFF-ON layer will be active in the left border of the bar, while the ON-OFF layer will be active on the right border of the bar. For the reversed intensity image (i.e., dark vertical bar on a light background), the OFF-ON layer will be active on the right border of the bar and the ON-OFF layer on the left. Thus, if the correlational operator is applied to distinct ON-OFF and OFF-ON layers, the cortical columnar image produced by a positive-negative RDS pair

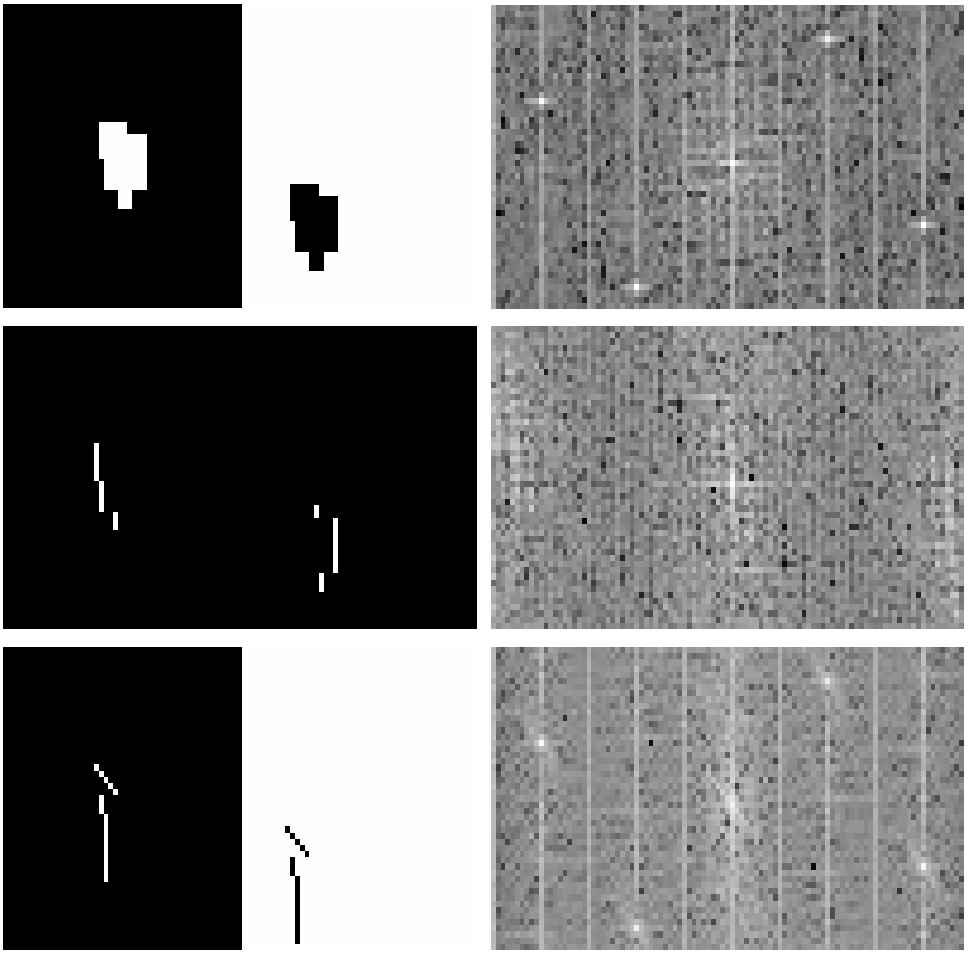

Fig. 2. Detection of disparity for positive-negative random dot pairs. *Top*: The left-right image patch (*left*) is a small section from a positive-negative random dot stereogram. On the *right* is the cepstrum of this image patch. The disparity can be easily detected by the position of the bright dots. *Middle*: The same image as above, but image patch preprocessed by a directional edge filter (e.g., OFF-ON) before applying the cepstrum. It can be seen that the disparity is no longer evident in the cepstrum. The transitions in the positive half of the stereogram do not match the transitions in the negative half when viewed after application of the OFF-ON filter. A similar result holds for an ON-OFF filter (not shown). *Bottom*: A line stereogram, viewed after the same OFF-ON filter applied above. Because of the coherent linear structure, the difference between the positive and negative halves of the stereogram is a coherent linear shift. For this case, the cepstrum clearly detects the stereo match, which the cepstrum failed to detect when the stereo pair was composed of random dots

differs in the spatial location of the edges, and the correlation (or cepstral) peak will be rather weak.

For line stereograms, this effect will not be sufficient to interfere with the correlational operator, since the line elements in the image are of considerable extent, yielding a constant "offset" that is correlated over the (long) length of the line elements. However, for random dot stereograms, which consist of many (short) line elements, the "offset" will be locally random and will interfere with the correlational operator. This effect is clearly evident in simulation, and in Fig. 2B the cepstral peak is not detectable due to the local randomization caused by the RDS line elements processed by an ON-OFF filter. We conclude that the separate processing of the ON-OFF and OFF-ON channels in primate vision is sufficient to allow a "square-law" type of stereo algorithm (auto/cross correlation or cepstral filter) to be consistent with existing experimental data on stereo vision.

4 Functional architecture in primate V-1

4.1 Magnification factor and the cortical map

In primates (and other higher vertebrates), the visual system is space-variant. Visual resolution, as well as many other functional aspects of vision, change in an orderly, monotonic fashion with increasing visual angle (measured from the fovea or direction of gaze). In turn, these phenomena depend on the underlying anatomical fact that the map of cortical position, as a function of retinal position, is strongly nonlinear. As the magnitude of the derivative of this map, which is called the cortical magnification factor (Daniel and Whitteridge 1961), is approximately inverse linear (Schwartz 1977b; Drasdo 1977), a two parameter fit to a 2D approximation of the cortical map is given by the complex logarithm function of the following form (Schwartz 1980):

$$w = K \log(z + a)$$

with w (cortical position) measured in millimeters, z (complex variable representing azimuth and eccentricity in the visual field in units of degrees), and a an experimental constant, which has been estimated to be around 0.3° (Dow et al. 1981; Schwartz 1985) to 1.0° (Tootell et al. 1982). The constant K in (1) may be determined from the (peak) cortical magnification at $z = 0°$, $K/a =$ peak magnification.

In macaques, the parameter a [in (1)] has been estimated to be 0.3° by Dow et al. (1981). Other studies have generally obtained larger values, such as Van Essen et al. (1984), who calculated roughly 0.7°, and Tootell et al. (1982, 1988), who estimated about 1°, although these same data were re-analyzed (Schwartz 1985) and a value of 0.3° obtained, in agreement with Dow et al. (1981). The precise magnitude of this constant a is not of great importance in the present context since we include several recent estimates of magnification factor, providing a band which brackets the psychophysical data of interest.

The value of peak magnification (K/a) in the central fovea, for macaques, has been estimated at 13 mm · deg^{-1} (Tootell et al. 1982), 16 mm · deg^{-1} (Van Essen et al. 1984), and 30 mm · deg^{-1} (Dow et al. 1981). The mean of these measurements is 20 mm · deg^{-1}. Obviously, there is an extremely large spread here, and it is difficult to weight these measurements since none of the papers cited above provide any quantitative error analysis.

Experimental work in this area began in the 1940s with Talbot and Marshall (1941). The observation that the inverse magnification factor was roughly linear, and hence that 2D cortical topography was approximately complex logarithmic, began in the late 1970s (Schwartz 1976, 1977b). Slightly later, a large number of papers began to appear linking psychophysical measurements to "cortical scaling" (see Wilson et al. 1990, for review). However, only very recently have there been attempts to account for the influence of the curvature of the cortical surface and the use of conformal mapping models which generalize the complex logarithm models (see Schwartz 1994, for review). This latter work has succeeded in placing error bounds on the two-dimensional conformal model, which are in the range of 10%–20%. Thus, by careful brain flattening and modeling techniques, it is possible to obtain quite precise models of cortical topography. Nevertheless, the range of estimates that exist in the field are quite wide, and as noted, usually unaccompanied by error analysis. Despite several human PET and fMRI studies (Schwartz et al. 1984; Fox et al. 1987; Sereno et al. 1995), we still do not have any precise direct measurement of human topography available and shall simply use an average of recent attempts to estimate the human magnification factor.

In this spirit, we will now summarize recent estimates for the human magnification factor. The value of peak magnification in the central fovea, for humans, has been estimated at 15 mm · deg^{-1} (Cowey and Rolls 1974), 11.5 mm · deg^{-1} (Drasdo 1977), 8 mm · deg^{-1} (Rovamo and Virsu 1979), and most recently, 20–25 mm · deg^{-1} (Tolshurst and Ling 1988). The mean is 14.3 mm · deg^{-1}. We will now use this estimate, together with measurements of human ocular dominance column spacing, to estimate λ_C.

4.2 Estimate of ocular dominance column and hypercolumn size in human V-1

In humans (Horton and Hedley-White 1984) and macaque monkeys (LeVay et al. 1975), the afferent input (layer IV) to the primary visual cortex is in the form of strips of left and right eye terminations (see Fig. 3). Human ocular dominance columns are about 1 mm wide (Horton and Hedley-White 1984) and monkey ocular dominance columns are both 0.5 mm wide. Within each strip (ocular dominance column), there is a topographic organization of a small region of the left or right eye (LeVay et al. 1975). The functional reason for the existence of these strips is at present unknown. Figure 3 shows a reproduction of the overall pattern of macaque ocular dominance strips, recon-

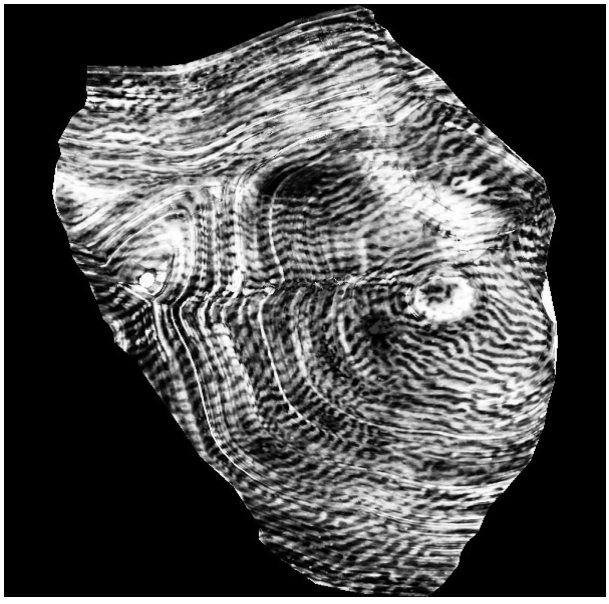

Fig. 3. Computer-flattened V-1 cortex of the macaque monkey: the data were obtained from a one-eyed monkey whose brain was subsequently stained with a metabolic marker (from Schwartz 1994). The periodic pattern of the ocular dominance column system is clearly visible. *Dark strips* represents image input from the left eye, *bright strips* input from the right eye. The strips are about 0.5 mm wide

structed from a cytochrome oxidase study of layer IV afferents following the enucleation of one eye of a macaque monkey, with subsequent computer brain flattening and reconstruction (Schwartz 1994).

We can estimate the angular extent of a pair of ocular dominance columns (one hypercolumn) in the human, corresponding to what Hubel and Wiesel (1974) have termed a "hypercolumn", or basic cortical processing module. This is

$$\lambda_C = 2\,\text{mm} \cdot (14.3\,\text{mm/deg})^{-1} = 0.14^\circ$$

or about 8 min of arc, using the above average estimate for human topographic mapping and estimates for human ocular dominance column size (Horton and Hedley-White 1984). Other workers (Schein and de Monasterio 1987; Wilson et al. 1990) have obtained similar estimates.

For purpose of comparison to psychophysical measurement, we will interpret this result in a "one-sided" sense, i.e., this is the maximum range to "one side" of a hypercolumn (see Fig. 4). The two-sided result is twice

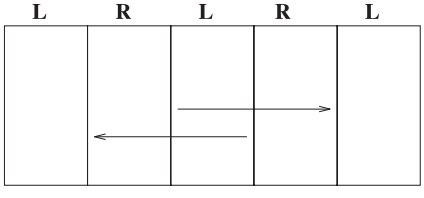

Fig. 4. Schematic representation of ocular dominance columns. The single-sided distance is depicted by *arrows*, representing 6–8 min of arc. The double-sided distance is twice as that

this, and we thus take an estimate of about 15 min of arc (foveal) to represent the "two-sided" λ_C.

It is evident from Fig. 3 that the pattern of cortical ocular dominance columns is roughly constant over nearly the entire cortex [although we note that Van Essen et al. (1984) have stated that column width decreases in the far periphery of the visual field]. Therefore, the angular extent of a pair of ocular dominance columns increases linearly with inverse cortical magnification. Clearly, if the ocular dominance column pattern has any simple relationship to stereopsis, the corresponding psychophysical quantities should scale linearly with cortical eccentricity. This is a corollary of the original hypercolumn concept of Hubel and Wiesel (1974), which defined a hypercolumn in terms of a pair of ocular dominance columns, and the associated length of a full set of 180 deg of orientation tuning, to provide a basic cortical module whose scale was invariant across the cortex and whose retinal size, therefore, increased linearly with eccentricity.

We will begin by establishing that a range of phenomena, including Panum's area (as measured by Ogle 1952), the variance of binocular vergence control reported by Motter and Poggio (1984) and Tyler's (Tyler 1974, 1977) observations on the limiting ability to resolve rapid changes in disparity are all consistent with a foveal limit provided by λ_C. Then, we will consider the evidence for the scaling of stereopis with cortical eccentricity, and use these discussions to provide a simple explanation for several related psychophysical phenomena.

5 Psychophysical correlates

5.1 Panum's fusional limit

Panum's area is classically defined as a small region of the visual field, over which stereo fusion is possible. Its magnitude is usually estimated at about 6–8 min of arc (foveal). It should be noted that this number represents the single-sided fusional area only, while the full (double-sided) area is therefore 12–16 min of arc (foveal). The concept of Panum's area has been called into question by several experiments. Fender and Julesz (1967) describe a hysteresis phenomenon in which there is a slow "pulling" apart of a fused stereo frame. Subjects can tolerate disparities of several degrees when the stimulus is slowly manipulated in this manner. Since hysteresis does not occur under normal viewing conditions, we do not discuss it further in this paper.

A more fundamental challenge to the notion of Panum's area comes from other experiments in which Panum's area has been found to be a function of the stimuli used rather than having a fixed (foveal) size. One term associated with this apparent negotiability of Panum's area is "disparity scaling" (Tyler 1974, 1977; Schor et al. 1989). In these experiments, it has been shown that larger stimuli have larger fusion ranges. In another experiment, Burt and Julesz (1980) introduced the term "disparity gradient" to describe apparent

complexities of fusion arising from the interaction of two nearby stereo stimuli. Put briefly, there are interactions between pairs of stereo targets when the ratio of their disparity to angular separation exceeds a certain amount. This quantity, and the phenomena associated with it, have been interpreted by Burt and Julesz (1980) to challenge the validity of the concept of Panum's area.

These apparent complexities of phenomenology of Panum's area have called into question the utility of the concept itself. If the area of fusion is a complex function of the stimulus used, then it is not clear that there is a well-defined angular size for Panum's area, much less whether it scales with cortical eccentricity! However, one of the principal results of the present paper is that both disparity scaling and the disparity gradient discussions of Julesz and Burt can be reconciled with a simple notion of a fixed Panum's area, of size λ_C in the foveal cortex. After presenting support for this statement, we will then present evidence that λ_C is a constant across the cortical surface, hence scales with cortical eccentricity in the same way as the inverse cortical magnification factor. The logic of this paper is to first present evidence that λ_C provides an estimate of several foveal phenomena of stereopsis. Then we will present evidence that the parafoveal and peripheral cortex is scaled in terms of the same constant λ_C.

5.2 A lower bound on the stereopsis window

Tyler (1977) quotes Wheatstone's (1838) observation that "stereopsis is reduced when the figures become too complex". In an important series of experiments, Tyler has quantified this observation by presenting human subjects with disparity gratings, which are stimuli whose binocular disparity varies sinusoidally. Using these stimuli, he has demonstrated that humans cannot process rapid changes in stereopsis. Tyler found this limit to be about 4–5 cycles/deg, which corresponds to a window of size 12–15 min of arc, within which disparity variation cannot be processed. We interpret these findings to indicate that a lower bound on the stereopsis window or quantization is roughly 10–15 min of arc (foveal) for the double-sided fusional area.

Tyler interpreted his findings in a similar manner to that of the present paper, since he states (Tyler, 1977): "[because] columns or strips of cells responding to similar orientations [are] very narrow compared to those responding to depth.."one would therefore expect the spatial integration across the cortex to be coarser for depth than for form processing."

Using our estimate for a single foveal hypercolumn, we can quantify Tyler's observations as being consistent with λ_C.

5.3 Binocular vergence error

Motter and Poggio (1984) have provided data showing that the accuracy of the binocular vergence system (macaque) is not better than 10–15 min of arc. The vergence pointing error is comparable to λ_C. Just as monocular micronystagmus adds a random error of about 1 min of arc, which is comparable to the monocular quantization size (i.e., to maximum visual acuity), the binocular fixation error is comparable to the binocular quantization size estimated from the present analysis.

5.4 Foveal and parafoveal magnitude of Panum's area

Ogle performed a classic series of experiments on the nature of stereopsis, and also provided a series of measurements on the dependence of stereopsis on angular distance from the fovea (Ogle 1952). In the fovea, the classical range over which stereo fusion occurs, called Panum's area, is in the range of 6–8 min of arc-disparity. Note that this measurement is the single-sided Panum's area, meaning that its full extent is 12–16 min of arc. Ogle's measurements indicate that Panum's fusional area scales linearly with eccentricity. Moreover, like many other visual parameters, Panum's area scales with eccentricity in a manner that fits the cortical magnification factor (Hampton and Kertesz 1983).

Combining Ogle's data and the observations of Hampton and Kertesz (1983), it is clear that the data for Panum's area are consistent with a basic cortical module, of size λ_C, independent of eccentricity. In other words, Ogle's data indicate that the range of fusion extends over a single cortical hypercolumn, and that this is true regardless of position in the visual field.

Hampton and Kertez's finding as well as Ogle's measurements of Panum's area and its dependence on visual eccentricity seem to be directly contradicted by a more recent experiment of Schor et al. (1986), which used stimuli of defined spatial frequency content to study the dependence of Panum's area on visual eccentricity. These apparently contradictory experimental reports may be resolved by a careful analysis of the differences in experimental design between Ogle (1952) and Schor et al. (1986). When these latter workers presented stimuli to their subjects at parafoveal visual eccentricities, they did not change the scale of the stimulus itself. They presented the same stereo stimuli, consisting of stereo pairs of a difference-of-Gaussian profile of frequency 0.3 c/deg and 6 c/deg, and a broad vertical bar of width 1.5 deg stimulus at eccentricities 0, 1.5, 3 and 5 deg. They found that Panum's area was a constant at all four eccentricities.

This experiment did not properly scale the stimulus elements, since the same DOG-shaped stimulus was used at all eccentricities, changing only the stereo separation. Thus, in cortical coordinates, the stimulus was composed of elements which were consistently decreasing in cortical spatial size as the same stimulus was shown at increasingly larger retinal eccentricities!

The problem outlined above, which may be summarized as the failure to properly scale the stimulus element

size when presenting nonfoveal stimuli, is common to several other experiments in this area. For example, Fendick (1983) studied the eccentricity dependence of stereoacuity, and Westheimer (1982) studied the eccentricity dependence of vernier acuity. In both of these experiments, stimulus elements making up the vernier and stereo targets (composed, for example, of a pair of 1 min of arc boxes) were not scaled to match local cortical spatial frequency tuning. Clearly, if one wishes to measure the eccentricity dependence of a stereo separation or vernier offset, then it is mandatory to scale the elements from which these stimuli are constructed. Otherwise, one is confounding two effects: the potential scaling of stereo or vernier separation, and the decreasing detectability of a constant-sized stimulus element as it is shifted into the periphery.

Finally, we cite a very recent result, published after submission of this paper, which indicates that peak detection frequency for "disparity corrugations" is 0.8 mm, after correction for the cortical magnification factor (Prince and Rogers 1998). In other words, sensitivity for disparity corrugation scales with the cortical magnification factor, and the basic "modular" spatial frequency corresponds to roughly 1 mm of cortex independent of position in the visual field.

5.5 Disparity gradient and disparity scaling explained by cortical scaling of fusion limits

We now briefly discuss two additional phenomena of human stereovision: disparity scaling and the disparity gradient experiment of Burt and Julesz (1980). We will demonstrate that if the range of fusion of human vision (Panum's area) is determined by a constant λ_C in the cortex, as we have suggested, then a simple explanation of these phenomena is possible, which reinstates the simple notion of Panum's area as a constant region independent of stimulus and experimental details.

5.6 Disparity scaling

The fusion of large stimuli unavoidably involves the nonfoveal cortex. The larger the stimulus, the larger are the visual eccentricities of the boundaries of the stimuli. If, as Ogle has shown, more peripheral regions of the cortex have a larger Panum's area, then it is not surprising that larger stimuli have larger Panum's areas. In fact, Schor et al. (1989, p. 833) suggest this same possibility to explain disparity scaling, but reject it because their earlier experimental results (Schor et al. 1986) indicated that Panum's area is a constant, independent of eccentricity. But we have shown that this observation is likely due to the lack of appropriate scaling of their stimuli. In other words, both the data and the analysis of Schor et al. (1986, 1989) are consistent with the possibility that disparity scaling is a phenomenon caused by the cortical magnification factor.

In order to make this more precise, it is necessary to have a detailed computational model of stereo fusion, which would allow predictions of the expected range of the relationship of stimulus structure to fusion. Though some computational considerations have been proposed (Koenderink and van Doorn 1976; Ludwig et al. 1994), such a complete model has not yet been constructed to our knowledge. In the absence of such a model, we point out, following the suggestion of Schor et al. (1986), that if Panum's area scales with cortical eccentricity, then this might well be the origin of disparity scaling. More insight into this idea is presented by the following cortical simulation of the Burt-Julesz disparity gradient experiment.

5.7 The Burt-Julesz disparity gradient experiment

Burt and Julesz (1980) performed an important experiment that has been influential in the modern interpretation of Panum's area. In this experiment, subjects were shown pairs of dots. Each pair of dots was

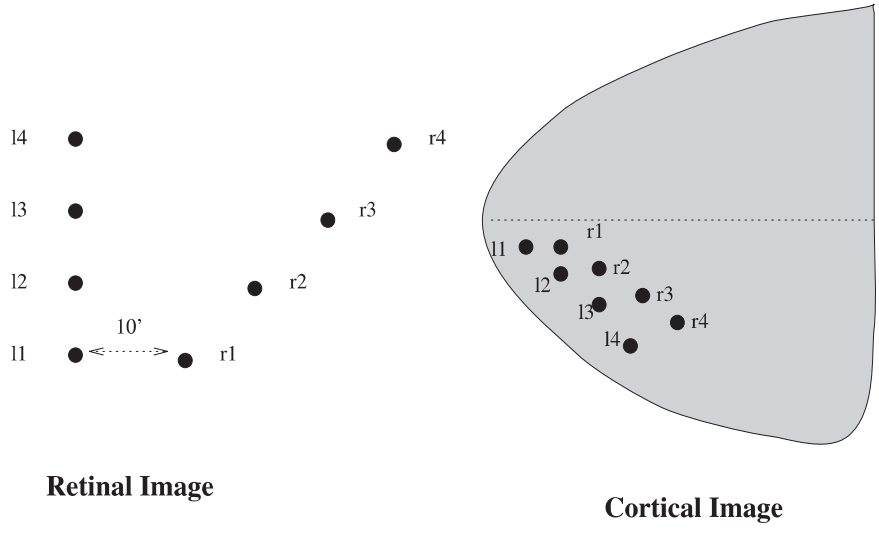

Fig. 5. Retinal (*left*) and cortical (*right*) representation of a pair of dots, illustrating the stimulus presentation of the disparity gradient experiment of Burt and Julesz (1980). *Left*: The retinal stimulus consists of four dots: l_1, r_1, and either pair of l_k, r_k, for $k = 2, 3, 4$. When fusion occurs, l_i is fused with the corresponding r_i. The retinal distance between l_1 and r_1 in this simulation is 10 min of arc. *Right*: Cortical representation of the input pattern on the *left*. Notice that the cortical distance between the two dots of all the pairs is almost constant

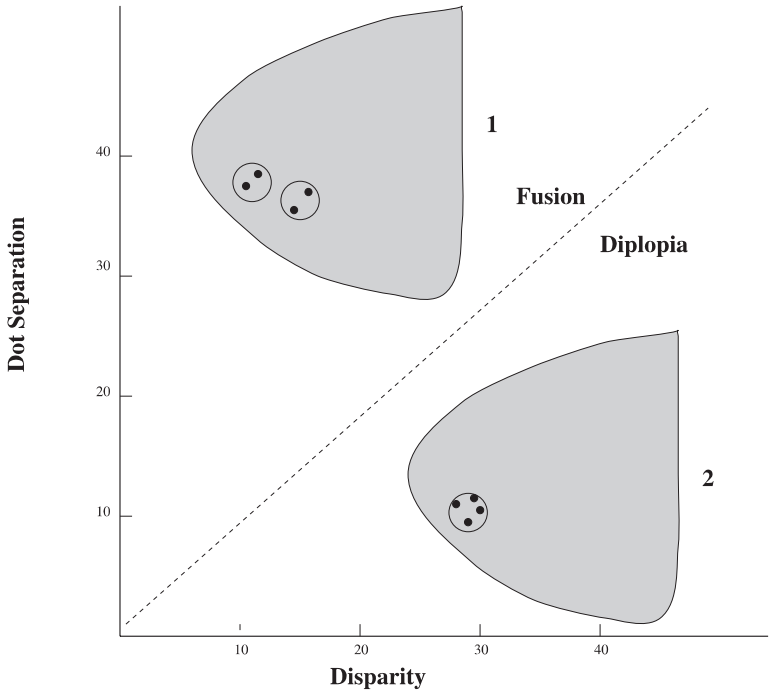

Fig. 6. Cortical representation (*1* and *2*) of the stimuli in the Julesz-Burt 'gradient disparity' experiment. The graph depicts areas of fusion (where spatial dot separation exceeds dot disparity) and areas of diplopia. In the original experiment, spatial separation between fusable two pairs of dots is reduced up to the point of diplopia. The *circles* represent a cortical 'patch' whose size is 12 min of arc (foveal). The cortical configuration of a fusable pair is depicted in *1*: the two pairs exceeds λ_C (the width of the circles). When the spatial dot separation is reduced (cortical configuration depicted in *2*), the two pairs fall within the same area of size λ_C, where only one disparity value can be perceived, therefore causing diplopia

parameterized by a disparity for each dot and an angular separation between the two dots (see Fig. 5A). It was found that the limiting disparity (i.e., Panum's limit) was not constant, but varied linearly with the distance between the pairs. In the actual experiment, only two pairs were presented in each trial, and in each consecutive trial the distance between pairs was reduced, until fusion was not possible.

Burt and Julesz (1980) defined the disparity gradient as the ratio of disparity difference to separation in visual space. They found that this disparity gradient measure was a good predictor of the ability of subjects to fuse the stimulus, independent of the classical notion of Panum's area. They concluded: "We have found that fusion is never obtained when the disparity gradient exceeds a critical value of approximately 1 (deg disparity)/(deg of dot separation). Thus, diplopia occurs even for dots with disparities well within the classical Panum's fusional area whenever the gradient limit is exceeded. It is this failure of fusion under normally favorable conditions that most clearly demonstrates the critical role of object interactions in fusion. It seems that nearby objects warp the fusional space, creating forbidden zones in which changes in disparity are too steep for fusion."

The results of the experiment deviate from the classical notion of Panum's limit in two ways:

1. The fusion limit increases with the distance between the pairs.
2. The fusion limit decreases below the classical value when the distance between the pair decreases below some threshold value.

However, both of these effects can be explained in terms of the cortical configuration of the stimuli used in this experiment, and using the classical concept of Panum's area. In order to explain (1) above, consider Figs. 5 and 6, where we show the schematic retinal and cortical configuration of the experiment. In order to show the cortical representation of the dots, we have used the model of cortical topography mentioned in (1). The two figures depict a simulation of the retinal-cortical mapping that we use in order to clarify our position. We show the central 1.2 deg of retinal and cortical representation of the pattern used by Burt and Julesz. The retinal distance between the two dots depicted as l_1 and r_1 in Fig. 5A is 10 min. The cortical patch size that represents about 12 min is depicted by the circles in Fig. 6. The precise details of the cortical map function are not critical to this discussion, merely the fact that cortical magnification is an approximately inverse-linear function of eccentricity whose magnitude is in the range estimated in this paper.

It is evident (see Fig. 5) that while the retinal disparity between the points increases, the cortical distance remains almost fixed. Thus, while the disparity limit is indeed changed in retinal coordinates, it remains fixed in cortical coordinates and stays below λ_C. In other words, an explanation of the disparity gradient phenomena does not require the assumption of a warping of binocular space, but merely an examination of the stimuli in their cortical representation. With two (stereo) stimuli, the set which is unavoidably further from the foveal representation will have a fusion limit which is somewhat larger (in retinal coordinates) than its pair.

The other limiting case of the disparity gradient experiment, (2) above, is explained by observing that when the two dots both have small disparities (compared to Panum's area), it is still possible for them to fail to be fused, provided that they are nearby in visual space. This is seen with reference to Fig. 6, where the cortical representations of the points in the Burt-Julesz disparity

gradient experiment are illustrated. Whenever the cortical representations of the two points are closer together than λ_C the binocular targets are NOT separated by a cortical window size of λ_C. But in this case, we expect there to be a failure of fusion based on Tyler's (1974, 1977) observations, as outlined in this paper. There is a minimum cortical separation which must be preserved to avoid interference with stereopsis. This amount is λ_C in Fig. 6, and it is capable of predicting the entire curve of the disparity gradient experiment, as shown in Fig. 5.

An earlier explanation of the Burt-Julesz experiment was suggested in a note added in proof to Schor and Tyler (1980): "[Burt and Julesz] have recently verified that disparity scaling of fusion limit applies to non-periodic stimuli in the form of a fixed gradient limit". This remark seems to be suggesting that the larger extent of the Julesz-Burt stimuli is expected to have a larger fusion range, and our explanation is based on a similar notion. However, we have explicitly related this to a quantitative model of the cortex, and also show that both phenomena of disparity scaling and disparity gradient may be explained on this single basis.

When the stimulus pairs are far apart, they are both capable of fusion by virtue of the increase in Panum's area with eccentricity. When the stimulus pairs are too close together, fusion fails by virtue of Tyler's observations on the limiting region over which disparity changes can be processed. Thus, the concept of a fusional area, whose size is about λ_C, and which scales with eccentricity, is sufficient to explain the results of the disparity gradient experiment.

6. Discussion

Two of the most prominent anatomical features of the primate visual cortex are the topographic mapping and interlacing of the left and right retina into a single binocular representation in layer IV of V-1. However, the relationship of these anatomical data and current psychophysical measurements of human stereopsis are much less explored. The original suggestion by Hubel and Wiesel (1974) that the size of a pair of ocular dominance columns determines a modular (hypercolumn) unit of striate cortex whose angular size in the retina would thus increase roughly linearly with eccentricity has resulted in a large amount of research aimed at determining the "cortical scaling" of various psychophysical phenomena. Curiously, it would seem that the origin of this idea, which lies in the constant width of ocular dominance columns across most of the surface of V-1, would have stimulated an analysis of cortical scaling and stereopsis. In particular, it would seem that stereo fusion, which has a classic modular structure in terms of Panum's area, would be a prime candidate for this analysis.

This has not been the case, and the reason can be traced to the series of experiments reviewed in this paper. In the first place, the very existence of Panum's area, and even of the concept of stereo fusion itself (Kaufman and Arditi 1976), has been called into question. Secondly, of the various experiments performed to study the variation of fusion limits with visual eccentricity, two are in agreement with cortical scaling (Ogle 1952; Hampton and Kertesz 1983), while Schor et al. (1986) explicitly contradicts it. However, we feel that we have presented a convincing argument that the data presented in Schor et al. (1986), when re-interpreted, suggest that Panum's area should in fact increase with visual eccentricity. Thus, we conclude that Panum's area is scaled by the size of a foveal hypercolumn, and increases in a linear fashion whose slope is comparable to most recent measurements of the cortical magnification factor.

Secondly, some of the puzzling phenomena of stereo fusion, such as disparity scaling and the Burt-Julesz disparity gradient experiment, can be interpreted by considering the stimulus configurations as they appear in V-1, together with the scaling of Panum's fusional limit with visual eccentricity.

Direct support for the existence of a modular basis for stereopsis greater than 8 min of arc has recently been described by Schlesinger and Yeshurun (1998). Analogous "modular" phenomena, also with a size in the range of λ_C, have been reported for monocular visual function. For example, the visual perception of texture (and probably motion) is an area, rather than point, process. This area must have a lower spatial limit (e.g., texture can be perceived on an area that is larger than the visual acuity). It is intriguing, in that regard, to mention that there are some preliminary indications that areas of size 8–12 min of arc determine a basic modular size for human texture analysis (Gagalowicz 1980; Or and Zucker 1989). It has also recently been found (Hermush and Yeshurun 1995) that a size limit exists on a human's ability to perceive more than a single motion vector, and it turns out that this limit is, again, about 10–12 min of arc.

Suggesting a mechanism of contour curvature detection, Wilson and Richards (1989) conclude that "at low curvature the visual system estimates curvature from contour orientation at sample points separated by 8.2 minutes of arc." Discussing interpolation of stereoscopic matches, Mitchison and McKee (1987) suggest that "the internal structure of grids of 5–7′ spacing must be available to the stereo matching system even for short durations".

While visual acuity is in the range of 1′, it seems that these experimental results, although varying from 5′–7′ to 10′–12′ (probably due to different experimental conditions), support our prediction (Yeshurun and Schwartz 1989) that visual data (and binocular visual data in particular) is processed, at least in an initial stage, on a coarser grid that has been shown to fit the size of a pair of ocular dominance columns, i.e., corresponds to the classical definition of a cortical hypercolumn (Hubel and Wiesel 1974).

The observations outlined in this work are significant for our understanding of the basic neural mechanisms of stereovision and also for computational approaches to machine vision. In fact, it appears that there are complex heuristic trade-offs in biological stereoscopic vision, such that extremely high stereoacuity is maintained, but that

the spatial complexity of stereo stimuli is compromised in terms of a fairly coarse quantization. At the present time, we do not know much about the detailed neural mechanisms responsible for stereopsis. However, a close study of the anatomical and psychophysical correlates of stereopsis represents a potentially important insight into both biological and computational stereovision.

References

Blake R, Wilson H (1991) Computational models of stereo vision. Trends in Neurosci 14

Bogert BP, Healy WJR, Tukey JW (1963) The frequency analysis of time series for echoes: cepstrum, pseudo-autocovariance, cross-cepstrum and saphe cracking. Proc Symp Time Series Anal p 209–243

Bracewell RN (1978) The Fourier transform and its applications. McGraw Hill, New York

Burt P, Julesz B (1980) A disparity gradient limit for binocular fusion. Science 208:615–617

Cowey A, Rolls ET (1974) Human cortical magnification factor and its relation to visual acuity. Exp Brain Res 3:447–454

Daniel M, Whitteridge D (1961) The representation of the visual field on the cerebral cortex in monkeys. J Physiol 159:203–221

Dow BM, Snyder AZ, Vautin RG, Bauer R (1981) Magnification factor and receptive field size in foveal striate cortex of monkey. Exp Brain Res 44:213–228

Drasdo N (1977) The neural representation of visual space. Nature 256:554–556

Fender DH, Julesz B (1967) Extensions of panum's fusional area in binocularly stabilized vision. J Opt Soc Am 57:819–830

Fendick M (1983) Effects of practice and the separation of test targets on foveal and peripheral stereoacuity. Vision Res 23:145–150

Fox PT, Miezin FM, Allman JM, Essen DCV, Raichle ME (1987) Retinotopic organization of human visual cortex mapped with positron emission tomography. J Neurosci 7:913–922

Gagalowicz A (1980) Visual discrimination of stochastic texture fields. Proc. 5th International Conference on Pattern Recognition, p 786–788

Hampton DR, Kertesz AE (1983) The extent of panum's area and the human cortical magnification factor. Perception 12:161–165

Hermush Y, Yeshurun Y (1995) Size limits on multiple motion perception. Perception 24:1247–1256

Horton JC, Hedley-White ET (1984) Cytochrome oxidase studies of human visual cortex. Philos Trans R Soc Lond [Bid] 304:255–272

Hubel DH, Wiesel TN (1974) Sequence regularity and geometry of orientation columns in the monkey striate cortex. J Comp Neurol 158:267–293

Jenkin MRM, Jepson AD (1989) The fast computation of disparity from phase differences. Conf. Computer Vision and Pattern Recognition, p 398–403

Julesz B (1971) Foundations of cyclopean perception. University of Chicago Press, Chicago

Kaufman L, Arditi A (1976) The fusion illusion. Vision Res 16:535–543

Koenderink JJ, Doorn van AJ (1976) Geometry of binocular vision and a model for stereopsis. Bio Cybern 21:29–35

Lee D, Mitra S, Krile TF (1989) Analysis of sequential complex images, using feature extraction and two dimensional cepstrum techniques. J Opt Soc Am [A] 6:863–870

LeVay S, Hubel DH, Wiesel TN (1975) The pattern of ocular dominance columns in macaque visual cortex revealed by a reduced silver stain. J Comp Neurol, 159:559–576

Ludwig KO, Neumann H, Neumann B (1994) Local stereoscopic depth estimation. Image Vision Comput 12:16–35

Marr D (1982) Vision. WH Freeman, New York

Mitchison GJ, McKee SP (1987) The resolution of ambiguous stereoscopic matches by interpolation. Vision Res 27:285–294

Motter BC, Poggio GF (1984) Binocular fixation in the rhesus monkey: spatial and temporal characteristics. Exp Brain Res 54:304–314

Ogle KN (1952) Disparity limits of stereopsis. Arc Opthalmol 48:50–60

Okajima K (1986) A mathematical model of the primary visual cortex and hypercolumns. Biol Cybern 54:107–114

Olson TJ, Potter RD (1988) Real-time vergence control. (Technical Report TR 264) University of Rochester

Or YH, Zucker S (1989) Texture fields and texture flows: sensitivity to differences in texture. Spatial Vision 4:131–139

Prince SJ, Rogers BJ (1998) Sensitivity to disparity corrugations in peripheral vision. Vision Research p 2533–2537

Rovamo J, Virsu V (1979) An estimation and application of human cortical magnification factor. Exp Brain Res 37:495–510

Schein SJ, Monasterio FM de (1987) Mapping of retinal and geniculate neurons onto striate cortex of macaque. J Neurosci 7:996–1009

Schiller PH (1983) Separate on/off pathways in retino-geniculate projection. Nature 297:580–582

Schlesinger B, Yeshurun Y (1998) Size limits on stereoscopic perception. Spatial Vision 11:279–293

Schor C, Tyler CW (1980) Spatio-temporal properties of panum's fusional area. Vision Res 21:683–692

Schor C, Wesson M, Robertson KM (1986) Combined effects of spatial frequency and retinal eccentricity on fixation disparity. Am J Optometry Physiol Optics 63:619–626

Schor C, Heckmann T, Tyler CW (1989) Binocular fusion limits are independent of contrast, luminance gradient and component phases. Vision Res 29:821–835

Schwartz EL (1976) Analytic structure of the retinotopic mapping and relevance to perception. 6th Annual Meeting of the Society for Neuroscience Abstracts, 6:1636

Schwartz EL (1977a) Afferent geometry in the primate visual cortex and the generation of neuronal trigger features. Biol Cybern 28:1–24

Schwartz EL (1977b) Spatial mapping in primate sensory projection: analytic structure and relevance to perception. Biol Cybern 25:181–194

Schwartz EL (1980) Computational anatomy and functional architecture of striate cortex: a spatial mapping approach to perceptual coding. Vision Res 20:645–669

Schwartz EL (1985) On the mathematical structure of the retinotopic mapping of primate striate cortex. Science 227:1066

Schwartz EL (1994) Computational studies of the spatial architecture of primate visual cortex: columns, maps, and protomaps. In: Peters A, Rocklund K (eds) Primary visual cortex in primates. (Vol 10 of Cerebral cortex) Plenum Press, New York

Schwartz EL, Christman DR, Wolf AP (1984) Human primary visual cortex topography imaged via positron-emission tomography. Brain Research 294:225–231

Sereno MI, Dale AM, Reppas JB, Kwong KK, Belliveau JM, Brady TJ, Rosen BR, Tootell RBH (1995) Borders of multiple visual areas in humans revealed by functional magnetic resonance imaging. Science 268:889–893

Tal D, Schwartz EL (1997) Computing with the leaky integrate and fire neuron: logarithmic computation and multiplication. Neural Comput 9:305–318

Talbot SA, Marshall WH (1941) Physiological studies on neural mechanisms of visual localization and discrimination. Am J Opthalmol 24:1255–1263

Tolshurst DJ, Ling L (1988) Magnification factors and the organization of the human striate cortex. Human Neurobiol 6:247–254

Tootell RB, Silverman M, Switkes E, deValois R (1982) Deoxyglucose analysis of retinotopic organization in primate striate cortex. Science 218:902–904

Tootell RBH, Hamilton SL, Silverman MS, Switkes E (1988) Functional anatomy of macaque striate cortex. 1. Ocular

dominance, binocular interactions, and baseline conditions. J Neurosci 8:1531–1568
Turner MR (1986) Texture discrimination by gabor functions. Biol Cybern 55:71–82
Tyler CW (1974) Depth perception in disparity gratings. Nature 251:140–142
Tyler CW (1977) Spatial limitations of human stereoscopic vision. Proc SPIE 120:36–42
Van Essen DC, Newsome WT, Maunsell JHR (1984) The visual representation in striate cortex of the macaque monkey: asymmetries, anisotropies, and individual variability. Vision Res 24:429–448
Virsu V, Rovamo J (1979) Visual resolution, contrast sensitivity and the cortical magnification factor. Exp Brain Res 37:474–494
Weinshall D (1989) Perception of multiple transparent planes in stereo vision. Nature 341:737–739
Westheimer G (1982) The spatial grain of the perifoveal visual field. Vision Res 22:157–162
Wilson H, Richards WA (1989) Mechanisms of contour curvature discrimination. J Opt Soc Am 6:106–115
Wilson H, Levi D, Maffei L, Rovamo J, DeValois R (1990) The perception of form. In: Spillman L, Werner W (eds) Visual perception: the neurophysiological foundations. Academic Press, New York
Yeshurun Y, Schwartz EL (1989) Cepstral filtering on a columnar image architecture: a fast algorithm for binocular stereo segmentation. IEEE Trans Pattern Anal Mach Intell 11:759–767